

Supporting Information

MATERIALS AND METHODS

The starting compounds, ruthenium chloride ($\text{RuCl}_3 \cdot x\text{H}_2\text{O}$), 2,2'-bipyridine-4,4-dicarboxylic acid (dcbpy), 2,4,6-trimercapto-1,3,5-triazine ($\text{C}_3\text{S}_3\text{N}_3\text{H}_3$ – tmt), trisodium citrate ($\text{Na}_3\text{C}_6\text{H}_5\text{O}_7 \cdot 2\text{H}_2\text{O}$ – cit) and tetrachloroauric acid (HAuCl_4) were purchased from Sigma-Aldrich. All the reagents employed were of analytical grade and used as supplied. Citrate-stabilized gold nanoparticles (*cit*-AuNP) were obtained according to the method introduced by Turkevich⁴⁵ and modified by Frens⁴⁶. They were always freshly prepared and monitored by UV-visible spectroscopy, dynamic light scattering (DLS) and hyperspectral microscopy. The UV-vis absorption spectra were recorded on a Hewlett Packard 8453A diode-ray spectrophotometer, in the 190 to 1100 nm range.

Analysis for $[\text{Ru}(\text{dcbpy})_2(\text{tmt})]\text{Cl} \cdot 4\text{H}_2\text{O}$ (MW = 801.4 g): C: 37.49; H: 3.07; N: 10.65; Calc. (%): C: 37.14; H: 3.00; N: 11.23. $^1\text{H-NMR}$ (ppm): $\text{H}(\alpha)=9.77$, $\text{H}(\alpha')=8.70$, $\text{H}(\beta)=7.96$, $\text{H}(\beta')=7.96$, $\text{H}(\delta)=8.80$, $\text{H}(\delta')=8.76$, $\text{H}(6)=7.79$, $\text{H}(6')=7.64$, $\text{H}(5)=7.34$, $\text{H}(5')=7.34$, $\text{H}(3)=8.63$ and $\text{H}(3')=8.61$. ESI-MS: $[\text{Ru}(\text{dcbpy})_2(\text{tmt})]^+=765.9$ m/z.

Theoretical Calculations: Geometry optimization was performed at the MM+ level using a conjugated gradient method implemented in the HyperChem Professional 8.05 program, adopting 1×10^{-7} kcal \AA^{-1} mol $^{-1}$ as the convergence criterion. SCF molecular orbital calculations were performed at RHF level using ZINDO/S method and the default parameters $k_{p\sigma} = 1.267$ and $k_{p\pi} = 0.585$. The electronic spectra were calculated considering single configuration interactions

(CI) in an active space of 20 frontier molecular orbitals (MO), 10 highest occupied and 10 lowest unoccupied MOs.

Table S1: Percent contribution of Ru(II), dcbpy and tmt wave functions on the MOs of complex (1), calculated by ZINDO/S.

| Molecular Orbital | Contribution per species | (%) |
|-------------------|--------------------------|-------|
| Ru | dcbpy | tmt |
| 109 | 0.04 | 99.83 |
| 110 | 0.06 | 99.81 |
| 111 | 0.08 | 99.91 |
| 112 | 0.05 | 99.92 |
| 113 | 0.04 | 99.84 |
| 114 | 0.07 | 99.81 |
| 115 | 77.77 | 16.94 |
| 116 | 71.8 | 19.43 |
| 117 HOMO | 60.15 | 36.11 |
| 118 LUMO | 0.43 | 30.73 |
| 119 | 6.58 | 65.64 |
| 120 | 11.20 | 86.46 |
| 121 | 0.59 | 1.90 |
| 122 | 1.43 | 98.00 |
| 123 | 1.96 | 97.58 |

| | | | |
|-----|------|-------|-------|
| 124 | 0.58 | 98.81 | 0.54 |
| 125 | 2.06 | 97.67 | 0.25 |
| 126 | 0.39 | 0.31 | 81.25 |

Table S2: Assignment of complex electronic spectra.

| λ_{\max} / nm | Assignment | Molecular Orbital | Oscillator Strength |
|-----------------------|---|--|---------------------|
| 248 | $n \rightarrow \pi^*$ | $112 \rightarrow 123$ | 0.0351 |
| 300 | | $116 \rightarrow 124$ | 0.0390 |
| 305 | $\pi \rightarrow \pi^*$ | $117 \rightarrow 123$ | 0.0481 |
| 369 | MLCT-1: Ru → dc _b H ₂ | $117 \rightarrow 124$ $117 \rightarrow 125$ | 0.1907 |
| 465 | MLCT-3: Ru → TMT | $115 \rightarrow 118$ | 0.1364 |
| 505-528 | MLCT-2: Ru → dc _b H ₂ | $117 \rightarrow 119$ $117 \rightarrow 118$ | 0.1132 0.0002 |

The pK_a values were determined by spectrophotometric titration of 3x10⁻⁵ mol L⁻¹ complex solution in H₂O/ethanol mixture (3:1 v/v) containing 0.5 molL⁻¹ NaCl as electrolyte, using a quartz cuvette. Three acid-base equilibria were registered in the pH 1 to 13 range.

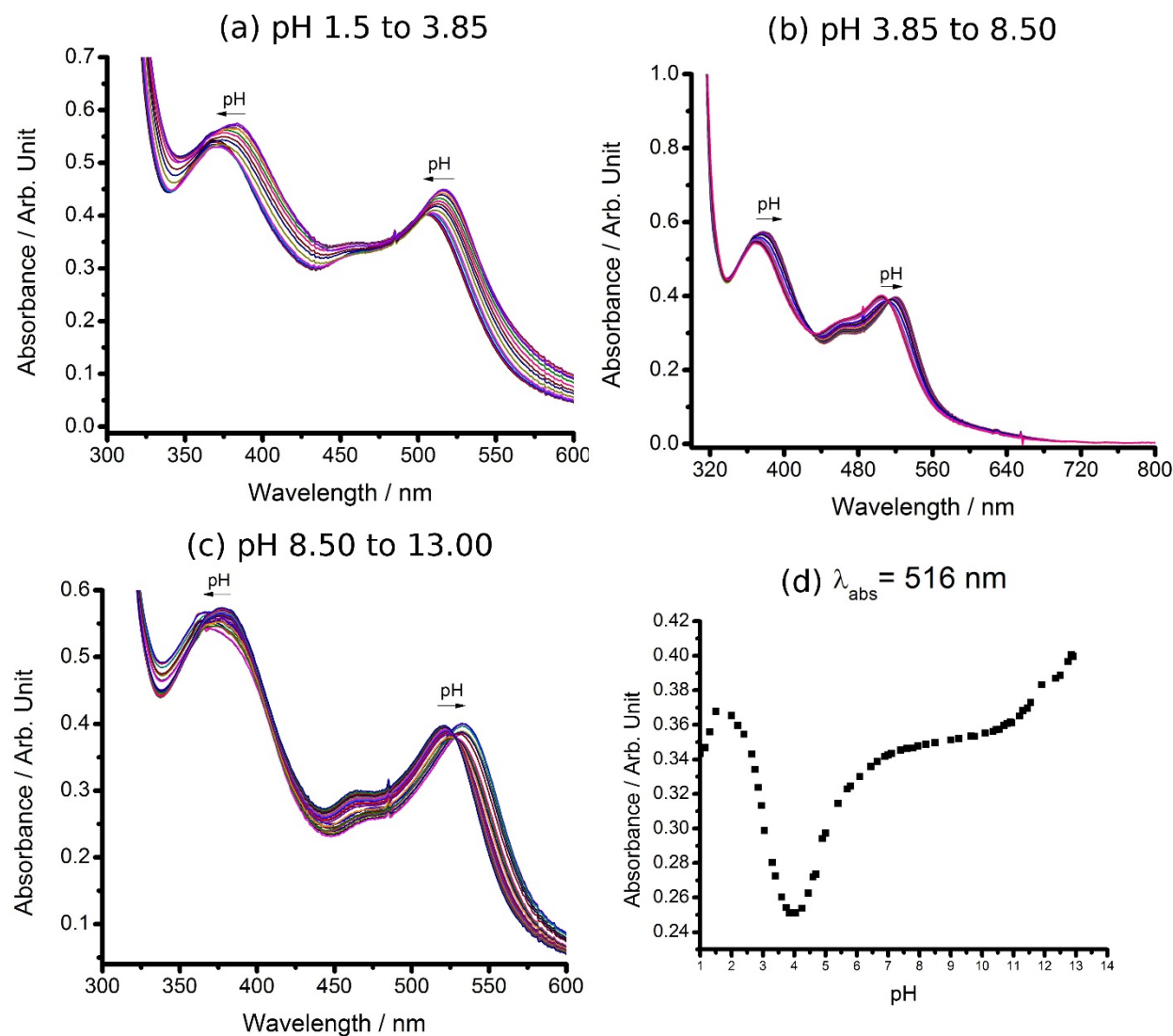


Figure S 1: Electronic spectra for the spectrophotometric titration in the range of pH 1.5 to 3.85

(a), 3.85 to 8.50 (b) and 8.50 to 13.0 (d). Plot of the absorbance at 516 nm as function of pH

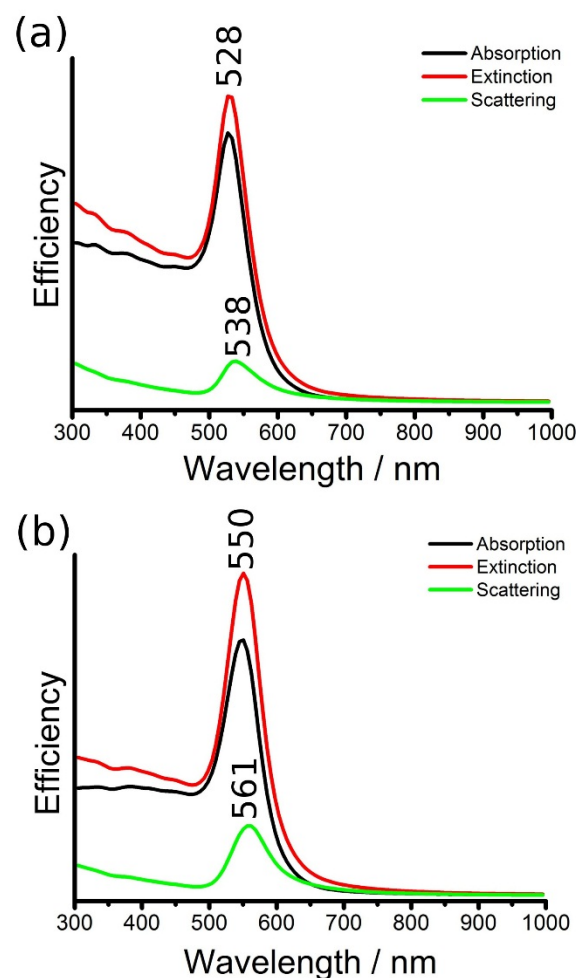


Figure S 2. Calculated absorption (black line), scattering (green line) an extinction (red line) spectra for spherical gold nanoparticles with 45 nm in water (a) an in silica with refractive index of 1.52 (b)

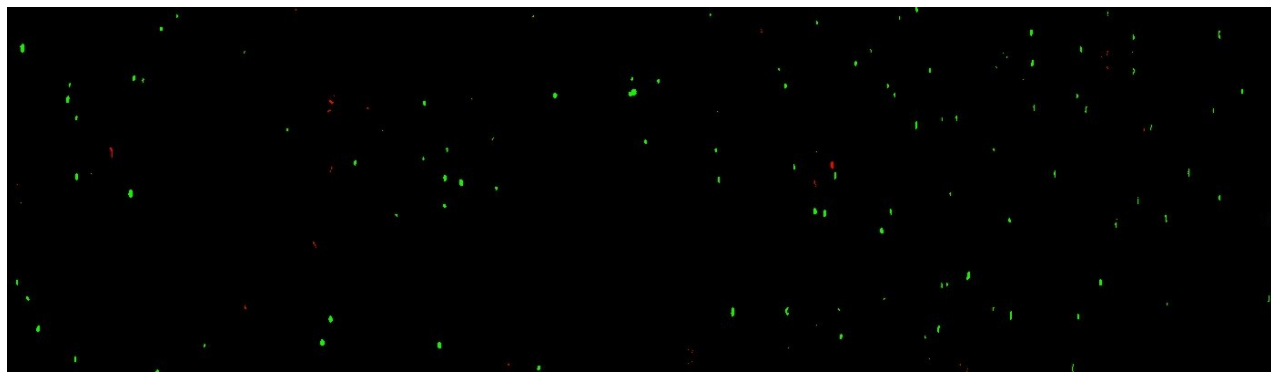


Figure S 3: Mapping image for AuNP-[Ru(dcbpy)₂(tmt)] immobilized on MPTS-coated glass.

The green dots pixels reflect scattering spectra of the isolated gold nanoparticles, and the few red dot pixels arise from the distinct scattering spectra the nanoparticle dimers.

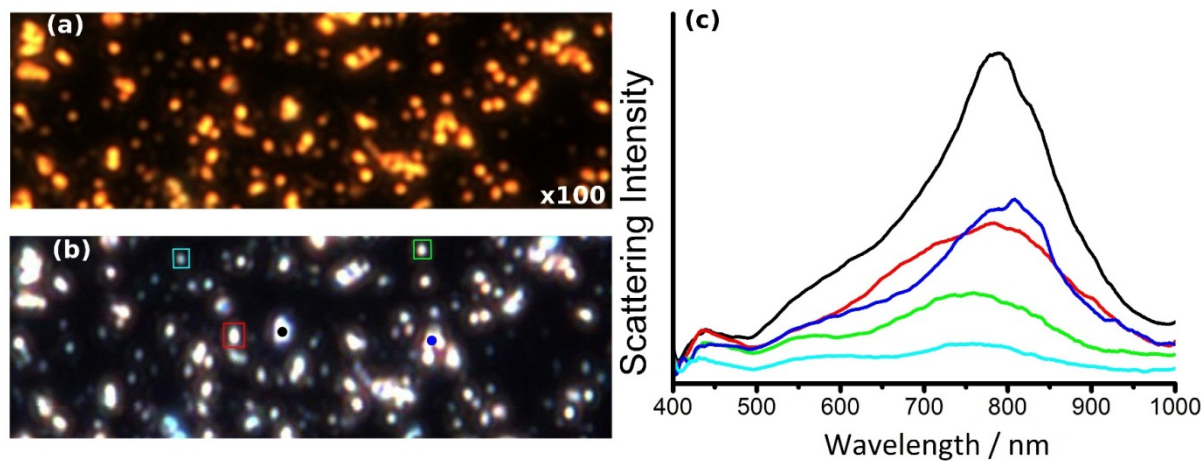


Figure S 4. Dark-field microscopy (a), hyperspectral image (b) and scattering spectra (c) of a sample prepared with Turkevich AuNP in the absence of the $[\text{Ru}(\text{dcbpy})_2(\text{tmt})]^{3-}$ complex, immobilized on a MPTS funcionalized glass. The spectral spots are indicated in Fig. S3b, with the corresponding colors of the scattering spectra.

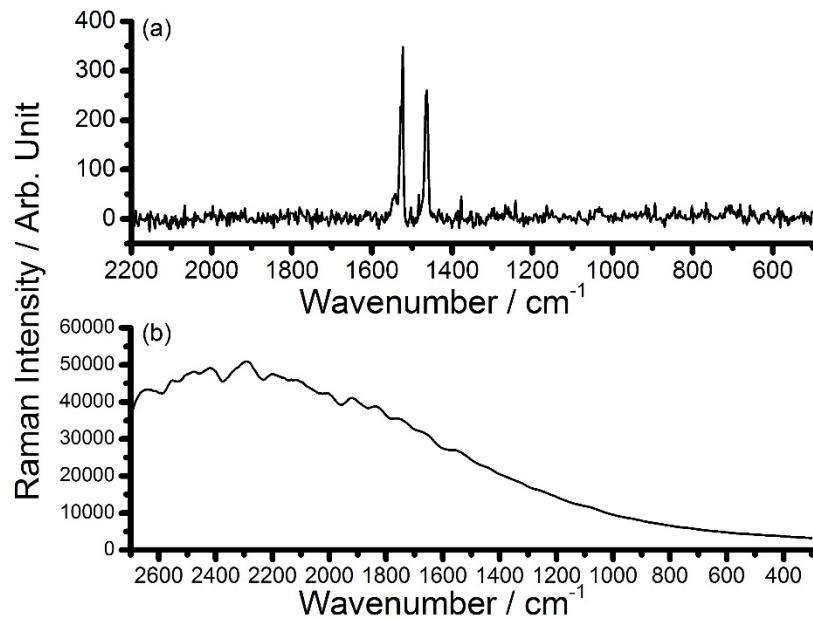


Figure S 5. Resonance Raman spectra of 2×10^{-5} mol L $^{-1}$ solution of $[\text{Ru}(\text{dcbpy})_2(\text{tmt})]^{3-}$ with excitation wavelength of 532 nm, laser power of 7.5 mW and integration time of 120s (a). Raman spectra of 10 mmol L $^{-1}$ solution of $[\text{Ru}(\text{dcbpy})_2(\text{tmt})]^{3-}$ recorded at 633 nm, laser power of 7.5 mW and integration time of 120s (b).

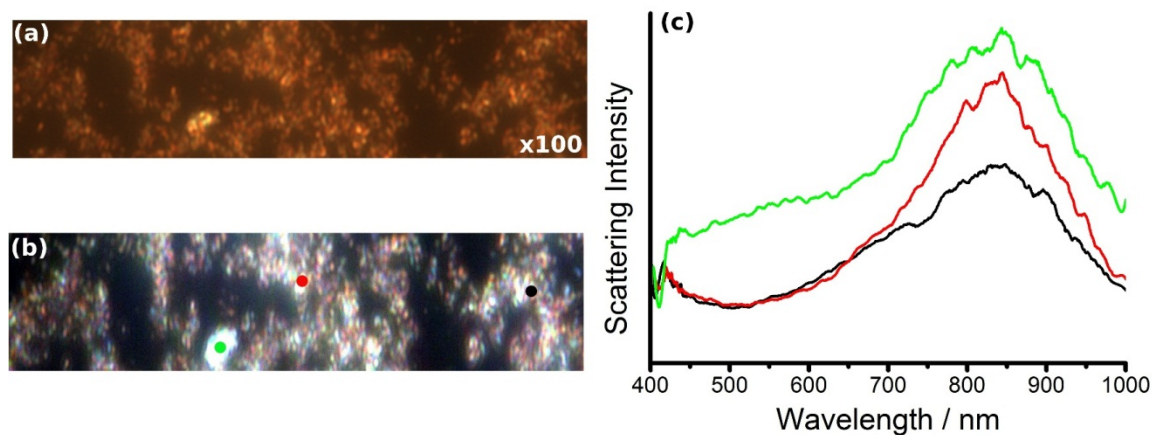


Figure S 6. Dark-field microscopy (a), hyperspectral image (b) and scattering spectra (c) of a sample prepared with agglomerated Turkevich AuNP ($+ \text{NaCl } 3 \text{ mmol L}^{-1}$) on MPTS functionalized glass.